Journal of Power Sources 264 (2014) 59–66

Contents lists available at ScienceDirect

Journal of Power Sources

journal homepage: www.elsevier.com/locate/jpowsour

Long-term durability of Ni/TiO_2 and $Ru–Ni/TiO_2$ catalysts for selective CO methanation

Shohei Tada [a,b], Ryuji Kikuchi [a,*], Katsuya Wada [c], Kazuo Osada [d], Kazuya Akiyama [d], Shigeo Satokawa [e], Yoshimi Kawashima [f]

[a] Department of Chemical System Engineering, Graduate School of Engineering, The University of Tokyo, 7-3-1 Hongo, Bunkyo-ku, Tokyo 113-8656, Japan
[b] Japan Society for the Promotion of Science, 5-3-1 Kojimachi, Chiyoda-ku, Tokyo 102-0083, Japan
[c] Toshiba Fuel Cell Power System Corporation, 2-4 Suehiro-cho, Tsurumi-ku, Yokohama-shi, Kanagawa 230-0045, Japan
[d] Nikki-Universal Co., Ltd., 7-14-1 Shinomiya, Hiratsuka-shi, Kanagawa 254-0014, Japan
[e] Department of Materials and Life Science, Faculty of Science and Technology, Seikei University, 3-3-1 Kichijoji-Kitamachi, Musashino-shi, Tokyo 180-8633, Japan
[f] Idemitsu Kosan Co., Ltd., 1280 Kami-izumi, Sodegaura, Chiba 299-0293, Japan

HIGHLIGHTS

- Durability Ni/TiO_2 and $Ru–Ni/TiO_2$ for selective CO methanation was studied.
- Ni/TiO_2 showed the long-term durability for 7000 h at a GHSV of 2500 h^{-1}.
- $Ru–Ni/TiO_2$ also exhibited high stability for 5500 h at a GHSV of 10,000 h^{-1}.
- NiO reduction was related with CO methanation activity and catalytic stability.

GRAPHICAL ABSTRACT

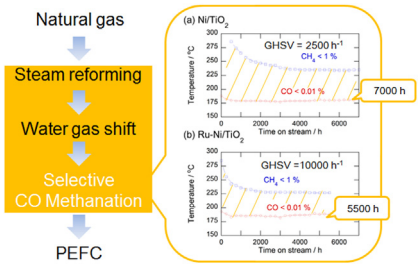

ARTICLE INFO

Article history:
Received 11 January 2014
Received in revised form
11 April 2014
Accepted 16 April 2014
Available online 26 April 2014

Keywords:
Long-term test
Nickel
Ruthenium
Titania: selective CO methanation
CO removal

ABSTRACT

Selective CO methanation was carried out over 10 wt%Ni/TiO_2 and 0.5 wt%Ru–10 wt%Ni/TiO_2, and the durability was examined. During the long-term test, both catalysts abated CO concentration from 0.25% (dry base) to less than 0.05% above ca. 175 °C with CO_2 methanation suppressed. $Ru–Ni/TiO_2$ exhibited the high activity of CO methanation compared to Ni/TiO_2 during the test. Furthermore, for more than 5500 h, $Ru–Ni/TiO_2$ maintained a wide temperature window for selective CO methanation (>50 °C), where CO and CH_4 concentrations were <0.05% and <1%, respectively, at a high gas hourly space velocity of 10,000 h^{-1}. Over Ni/TiO_2 and $Ru–Ni/TiO_2$, CO_2 methanation activity was initially enhanced, and then stabilized. The initial promotion of CO_2 methanation activity is possibly due to the reduction of NiO which remained unreduced after the prereduction by H_2 at 450 °C.

1. Introduction

In Japan, from 1980's, fuel cells have been regarded as a promising power generator with high efficiency and low environmental impact. They directly convert chemical energy into electrochemical energy and omit the intermediate steps of producing heat and mechanical power works of the most conventional power

* Corresponding author. Tel./fax: +81 3 5841 1167.
E-mail address: rkikuchi@chemsys.t.u-tokyo.ac.jp (R. Kikuchi).

http://dx.doi.org/10.1016/j.jpowsour.2014.04.075
0378-7753/

generation method. Polymer electrolyte fuel cells (PEFCs) are expected to be in the practical applications such as power sources for domestic uses and electric vehicles, and so on. In Japan, PEFC systems have been commercially available since 2009, and 50,000 units will have been installed by fiscal year 2013 [1]. The retail price of the PEFC system is gradually decreased, but remains expensive for domestic facility. In order to spread the PEFC systems, it is necessary to manufacture PEFC at a low cost and in large numbers. The following 4 topics have been studied all over the world for the significant cost reduction of the full-fledged commercialization of residential PEFC co-generation systems: a development of durable electrolyte materials, a development of CO tolerant anode catalysts, a development of CO removal processes from reformates, and a method to estimate the influence of impurities on fuel cell performance. As will be seen, this paper focuses on the CO removal processes by selective CO methanation.

PEFCs produce electric energy via the oxidation of hydrogen. Since hydrogen is requisite to attain high power density and efficiency with PEFCs, it is important to design catalytic process for hydrogen production from conventional fuels such as natural gas, liquefied petroleum gas (LPG), kerosene, and so on. As one of the problems for catalytic reforming processes, carbon monoxide (CO) in the reforming gases poisons the anode of the PEFCs operating at such low temperatures (ca. 80 °C). It is, therefore, imperative to reduce the CO concentration to below at least 100 ppm [2,3]. The CO concentration in the reformates can be reduced from ca. 10% to 0.2–2% by the water gas shift reaction (WGS reaction, $CO + H_2O \rightarrow CO_2 + H_2$) [4–6]. Following this, one alternative for decreasing the CO level is the preferential oxidation of CO (PROX) in the presence of excess H_2 ($CO + 1/2O_2 \rightarrow CO_2$) [7–10]. However, during PROX hydrogen is also easily oxidized in the presence of oxygen, leading to a decrease in the PEFC energy conversion efficiency.

Removal of CO by methanation ($CO + 3H_2 \rightarrow CH_4 + H_2O$, $\Delta H_{298}^\circ = -206$ kJ mol^{-1}) in the presence of excess CO_2 has been investigated. Alternation from PROX to CO methanation has the following advantages: no externally-supplied reactants and reuse of produced CH_4 as a heating fuel for the reforming units. On the other hand, the alternation causes a problem about simultaneous CO_2 methanation ($CO_2 + 4H_2 \rightarrow CH_4 + 2H_2O$ (g), $\Delta H_{298}^\circ = -165$ kJ mol^{-1}) and reverse water gas shift reaction (RWGS reaction, $CO_2 + H_2 \rightarrow CO + H_2O$ (g), $\Delta H_{298}^\circ = 41$ kJ mol^{-1}), leading to huge consumption of produced H_2 and runaway of a methanation reactor. It is, therefore, necessary to develop new catalysts which improve CO methanation at low temperatures and suppress CO_2 methanation and RWGS reaction at high temperatures. In addition, enhancement of low-temperature activity of CO methanation decreases the loading amount of methanation catalysts, resulting in downsizing CO removal units and, in consequence, cutting down the manufacture's cost. Taking into account application to CO removal units in commercial PEFC systems, the catalysts are also required to be stable for a long time.

A great deal of effort has been made in studies of selective CO methanation in the presence of CO_2 and H_2O over Ru–Ni monometallic and bimetallic catalysts [11–14]. Recently Chen et al. have reported that 1 wt%Ru catalysts supported on mesoporous Ni–Al oxides (33 and 40 mol% Ni) exhibited high activity and selectivity in CO methanation [13]. Furthermore, a durability test was carried out using these catalysts, and the catalyst has been stable for more than 200 h. In order to put into practical use, sophisticated catalysts with high durability (>60,000 h) and high activity and selectivity of CO methanation should be developed.

In our previous work, the effect of Ru particle size and support materials on selective CO methanation over Ru/Al_2O_3 and Ru/TiO_2 was studied [15]. Firstly, a close correlation was found between CO_2 conversion rate and perimeter length between Ru particles and supports, which indicates that the interface was reaction sites of CO_2 methanation in CO and CO_2 co-existing atmosphere. Secondly, CO_2 methanation over Ru/TiO_2 was suppressed in spite of long perimeter compared to Ru/Al_2O_3, stemming from the small amount of CO_2 adsorbed onto Ru/TiO_2. Using the information, Ni/TiO_2 [16] and $Ru–Ni/TiO_2$ [17–19] were developed for selective CO methanation catalysts, and exhibited high activity and selectivity of CO methanation. Catalysts for selective CO methanation are required to have a wide temperature window at a low temperature range for application to CO removal units in commercial PEFC systems, and the developed catalysts was located with a slight expansion of the window, as shown in Fig. 1. As for $Ru–Ni/TiO_2$, the introduction of Ni into Ru/TiO_2 decreased the CO_2 conversion rate. The Ru species were in close proximity to Ni species, leading to decrease in direct contact between Ru and TiO_2 and suppression of CO_2 methanation. However, little is known about the long-term durability. In this work, long-term tests of selective CO methanation was carried out over developed Ni/TiO_2 and $Ru–Ni/TiO_2$, and the durability of the catalysts was investigated.

2. Experimental

2.1. Catalyst preparation

0.5 wt%Ru–10 wt%Ni/TiO_2 catalysts were prepared by a co-impregnation method, and 10 wt%Ni/TiO_2 catalysts by an impregnation method. The TiO_2 support (Degussa P25) was impregnated with an aqueous solution of $Ru(NO_3)_3$ (Furuya Metal, 3.79% as Ru), and $Ni(NO_3)_2 \cdot 6H_2O$ (Wako, 98%). After impregnation all samples were dried at 120 °C and then calcined at 500 °C for 3 h in air.

2.2. Activity test

The long-term tests for selective CO methanation were carried out in a fixed-bed tubular reactor at atmospheric pressure. 40 g of Ni/TiO_2 or 10 g of $Ru–Ni/TiO_2$ was placed in the reactor, and then reduced at 450 °C for 3 h in 20% H_2/N_2 flow prior to each run. The feed gas, which simulates the methane reformate equilibrated at 190 °C, consists of 0.200% CO, 16.1% CO_2, 65.3% H_2 and 18.4% H_2O (dry base: 0.245% CO, 19.7% CO_2, 80.0% H_2). The gaseous mixture was fed at a gas hourly space velocity (GHSV) of 2500 h^{-1} (Ni/TiO_2)

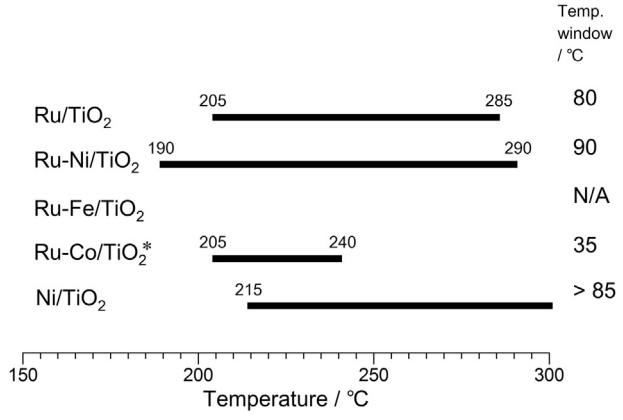

Fig. 1. Temperature window for selective CO methanation over 0.5 wt%Ru/TiO_2, 0.5 wt%Ru–5 wt%Ni/TiO_2, 0.5 wt%Ru–5 wt%Fe/TiO_2, 0.5 wt%Ru–5 wt%Co/TiO_2, and 5 wt%Ni/TiO_2. Catalyst preparation: wetness impregnation method for Ru/TiO_2 and Ni/TiO_2 catalysts using metal nitrate solution and TiO_2 (Degussa, P25), and wetness co-impregnation method for the others. Reaction condition: $CO/CO_2/H_2/H_2O = 0.154/15.5/62.3/22.0$, GHSV = 11,000 h^{-1}. Definition of window: CO concentration <500 ppm and CH_4 concentration <5000 ppm. * CO concentration <200 ppm and CH_4 concentration <5000 ppm [17,18].

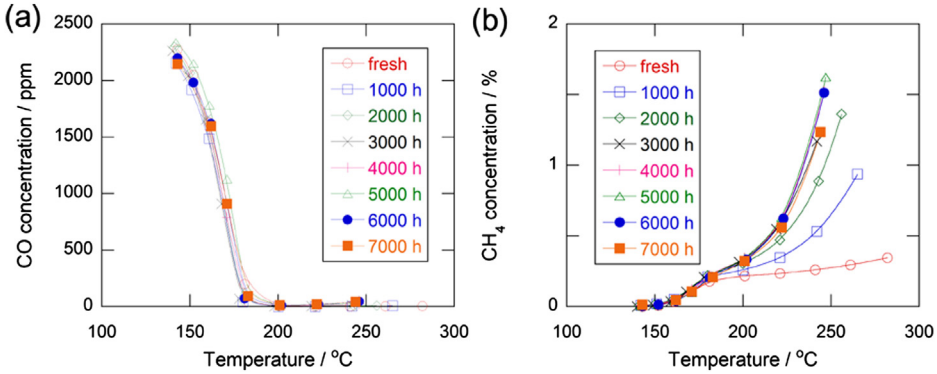

Fig. 2. Dependency of (a) CO and (b) CH_4 concentrations on reaction temperatures over 10 wt%Ni/TiO_2 after 0–7000 h of long-term test for selective CO methanation at 200 °C. Reaction condition: $CO/CO_2/H_2/H_2O$ = 0.2/16.1/65.3/18.4, GHSV = 2500 h^{-1}.

or 10,000 h^{-1} (Ru–Ni/TiO_2). The gas composition at the reactor outlet was analyzed with an infrared gas analyzer (Shimadzu, CGT-7000). At a certain time interval, the dependence of CO and CH_4 concentrations on reaction temperature was measured to evaluate the degree of the catalyst degradation.

Catalytic activities of CO_2 methanation were also measured in a 4-mm I. D. fixed-bed quartz tubular reactor at atmospheric pressure. 300 mg of catalysts was placed in the reactor. Prior to each catalytic measurements, the catalysts were reduced in 5% H_2/Ar at 450 °C for 0.5 h. A pre-mixed gas containing 20% CO_2/H_2 was introduced into the system, and was fed at a GHSV of 10,000 h^{-1}. The gaseous effluent was analyzed using a micro gas chromatograph (Varian, CP-4900) equipped with MS-5A, COX and PPQ columns and a thermal conductivity detector (TCD).

The outlet gas concentrations were described on the basis of the dry gas composition.

2.3. Characterization

The crystalline phase of catalysts was determined by X-ray diffraction (XRD) (Rigaku, Ultima IV) at voltage of 40 kV and current of 40 mA. X-ray photoelectron (XP) spectra were obtained with a JEOL JPS-90SX spectrometer using MgKα radiation. The binding energy in each XP spectroscopy measurement was referenced to the C 1s peak (285.0 eV). Scanning transmission electron microscopy (STEM, Hitachi HD-2000 STEM) was used to determine the morphology of the Ni particles on the catalysts. At the same time, X-ray energy dispersive spectrometry mapping (EDS mapping) was also measured. Temperature programmed reduction by H_2 (H_2-TPR) was carried out in a flow system (Quantachrome, CHEMBET-3000). About 30 mg of as-prepared samples was placed in the quartz tube, flushed initially with He flow at 300 °C, and cooled to room temperature. A gaseous mixture of 5% H_2/Ar was fed to the reactor at 30 ml min^{-1}. The temperature was raised at a heating rate of 10 °C min^{-1}. In order to investigate the reducibility of Ni species on Ni/TiO_2, H_2-TPR experiments was conducted for Ni/TiO_2 reduced at 450 °C for 30 min in the quartz tube. The outlet gases were analyzed by a thermal conductivity detector (TCD).

3. Results and discussion

3.1. 10 wt%Ni/TiO_2

The catalytic stability of 10 wt%Ni/TiO_2 for selective CO methanation was investigated on stream for 7000 h at 200 °C. At a constant time interval during the long-term test in the simulated reformates, CO and CH_4 concentrations were measured by changing the reaction temperature using the same apparatus of the long-term test. The temperature dependence of CO and CH_4 concentrations is plotted in Fig. 2. In Fig. 2(a), there was no difference among the CO concentration curves of the all data. Over all data, the CO concentration dropped rapidly with increasing temperature, and approached almost zero at 180 °C. No CO production was detected at high temperatures, which means that the reaction rate of CO methanation is faster than that of RWGS reaction.

As shown in Fig. 2(b), over all data CH_4 concentration increased up to 180 °C and then steady at ca. 2500 ppm. The CH_4 concentration balanced the initial concentration of CO (2450 ppm). The CH_4 concentration rose again at the temperatures above 200 °C. It is reported that residual CO suppressed CO_2 methanation even at quite small levels [17,20]. These indicate that CH_4 production at low temperatures occurred via CO methanation and at high temperatures via CO_2 methanation. The fresh Ni/TiO_2 catalyst hardly methanated CO_2, as indicated by the little increase in CH_4 concentration above 200 °C. The activity of CH_4 production was enhanced with increasing the reaction time up to 3000 h, and then became almost constant.

The CO_2 conversion and CH_4 selectivity for CO_2 methanation over the fresh and spent Ni/TiO_2 catalysts were investigated, as shown in Fig. 3. After 7000 h of operation, the spent catalyst was taken out from the reactor for evaluation. Prior to the catalyst performance evaluation, the fresh and spent catalysts were reduced at 450 °C for 30 min in the apparatus for CO_2 methanation. CO_2 conversion and CH_4 selectivity are defined as follows:

$$CO_2 \text{ conversion} = 1 - \frac{F_{CO_2,out}}{F_{CO_2,in}} \quad (1)$$

$$CH_4 \text{ selectivity} = \frac{F_{CH_4,out}}{F_{CO,out} + F_{CH_4,out}} \quad (2)$$

where $F_{x,in}$ and $F_{x,out}$ are the inlet and outlet molar flow rates of x species, respectively. After the long-term test of 7000 h, the CO_2 conversion was enhanced, as shown in Fig. 3(a). The CH_4 selectivity was almost 100% and slightly decreased to 99% after 7000 h of operation. The rest of converted CO_2 existed as CO, meaning that CO was produced by RWGS reaction. The production rates of CH_4 at 350 °C over the fresh and spent catalyst were 3.9 and 15 ml min^{-1} g_{cat}^{-1}, respectively. It is, thus, concluded that the long-term operation for 7000 h promoted RWGS reaction, leading to significant enhancement of CO_2 methanation activity.

3.2. 0.5 wt%Ru–10 wt%Ni/TiO_2

Fig. 4 shows the changes of CO and CH_4 concentrations over Ru–Ni/TiO_2 after 0–5500 h of operation at various reaction

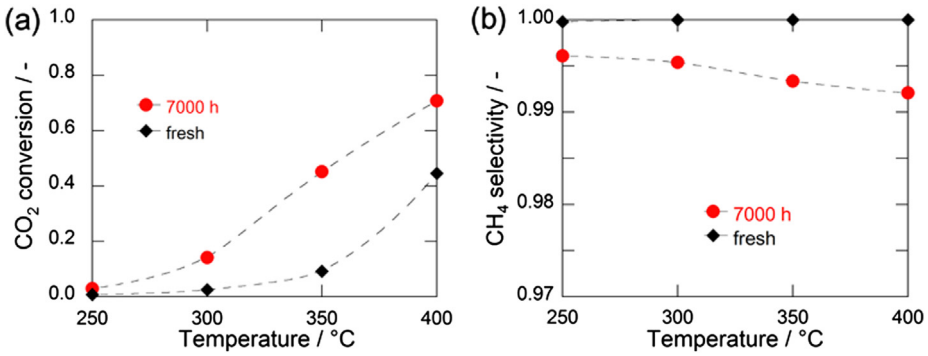

Fig. 3. (a) CO_2 conversion and (b) CH_4 selectivity over 10 wt%Ni/TiO_2 as-prepared and spent for 7000 h for selective CO methanation at 200 °C. Reaction condition: CO_2/H_2 = 20/80, GHSV = 10,000 h^{-1}. Prereduction: 450 °C for 30 min under 5% H_2/Ar.

temperatures. These long-term tests using Ru–Ni/TiO_2 were carried out at high GHSV (10,000 h^{-1}) compared to Ni/TiO_2 (2500 h^{-1}). The tendency of Ru–Ni/TiO_2 was similar to Ni/TiO_2, as shown in Figs. 2 and 4: CO concentration curve was unchanged and CH_4 production at high temperatures was boosted with increasing elapsed time. In Figs. 2(a) and 4(a), the decrease in the CO concentration of Ru–Ni/TiO_2 was faster than that of Ni/TiO_2 in spite of the high GHSV, which means that Ru–Ni/TiO_2 exhibited much higher activity for CO methanation than Ni/TiO_2. In Fig. 4(b), CH_4 concentration of the fresh catalyst was slightly increased with temperature, whereas over the Ru–Ni/TiO_2 after using more than 1000 h the CH_4 concentration was rapidly increased above 200 °C. It is noteworthy that the spent Ru–NiTiO_2 showed the almost the same curve of the CH_4 concentration to the spent Ni/TiO_2.

The CO_2 conversion and CH_4 selectivity for CO_2 methanation over the fresh and spent Ru–Ni/TiO_2 catalysts were plotted against reaction temperature in Fig. 5. The spent catalyst, which was taken out from the reactor for the long-term test, exhibited the higher CO_2 conversion than the fresh one. In addition, both catalysts displayed high selectivity to CH_4 (>99.8%) above 250 °C. According to these results, the long-term operation for Ru–Ni/TiO_2 boosted RWGS reaction, as is common with Ni/TiO_2 (Fig. 3). The activity for RWGS reaction over Ru–Ni/TiO_2 was rapidly enhanced compared to Ni/TiO_2.

3.3. Characterization

3.3.1. XRD

To investigate the change of the crystalline phases of Ni and Ru species and TiO_2 during the long-term test, powder XRD measurements of Ni/TiO_2 and Ru–Ni/TiO_2 were performed, as illustrated in Fig. 6. Both rutile and anatase phases were identified in the catalysts and the XRD patterns for the samples were unchanged by the long-term test. Peaks assignable to NiO at 43°, metallic Ni at 45 and 52°, and $NiTiO_3$ at 33, 36, and 41° were observed. After the durability test, the $NiTiO_3$ peaks disappeared. The mean crystallite size of metallic Ni was estimated from the XRD patterns using the Scherrer equation,

$$D = \frac{K\lambda}{\beta \cos\theta} \tag{3}$$

where K is the shape factor (0.89), λ is X-ray wavelength (0.154 nm), β is the line broadening at half the maximum intensity in radians, and θ is Bragg angle [21]. In Table 1, the crystallite size of metallic Ni on reduced Ni/TiO_2 was 22 nm, and almost the same as that of the spent Ni/TiO_2. The size on reduced Ru–Ni/TiO_2 was 7 nm and was unchanged by the long-term test. No Ru peaks were detected in the XRD patterns of Ru–Ni/TiO_2, indicating that Ru species are in amorphous state or that the Ru particle size is smaller than the XRD limit.

3.3.2. STEM

As illustrated in Fig. 7, scanning transmission electron microscopy (STEM) and energy dispersive spectroscopy (EDS) maps were used to study the Ni/TiO_2 and Ru–Ni/TiO_2. Fig. 7(a) and (c) display large fractions of Ni particles (average ca. 20 nm) on Ni/TiO_2 and Ru–Ni/TiO_2 catalysts after H_2 reduction, respectively. After 7000 h of operation, small Ni particles on Ni/TiO_2 were rather sintered and the small ones of size less than 10 nm were disappeared, shown in Fig. 7(b).

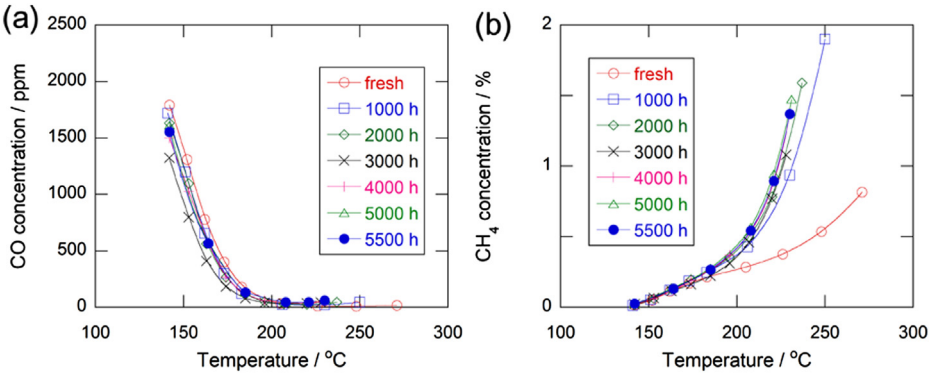

Fig. 4. Dependency of (a) CO and (b) CH_4 concentrations on reaction temperatures over 0.5 wt%Ru–10 wt%Ni/TiO_2 after 0–5500 h of long-term test for selective CO methanation at 200 °C. Reaction condition: $CO/CO_2/H_2/H_2O$ = 0.2/16.1/65.3/18.4, GHSV = 10,000 h^{-1}.

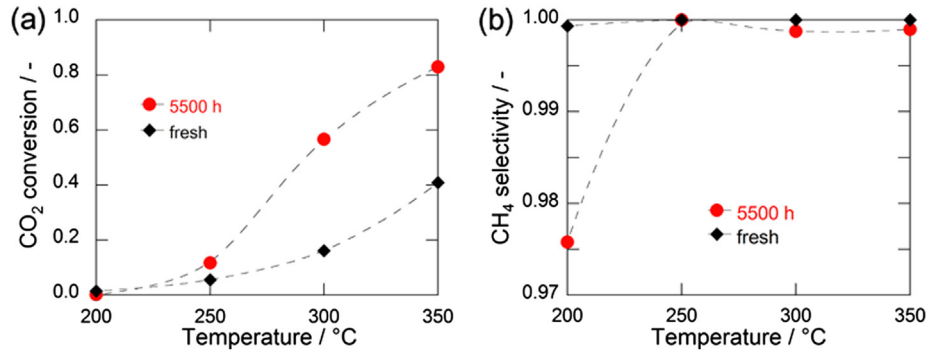

Fig. 5. (a) CO_2 conversion and (b) CH_4 selectivity over 0.5 wt%Ru–10 wt%Ni/TiO_2 as-prepared and spent for 5500 h for selective CO methanation at 200 °C. Reaction condition: CO_2/H_2 = 20/80, GHSV = 10,000 h^{-1}. Prereduction: 450 °C for 30 min under 5% H_2/Ar.

3.3.3. XP spectroscopy

Fig. 8 presents the Ni $2p_{3/2}$, O 1s, and Ti 2p XP spectra for Ni/TiO_2 and Ru–Ni/TiO_2. In Fig. 8(a), the XP spectra of Ni $2p_{3/2}$ can be divided into three peaks using a FWHM of 2.5 eV. The peaks at 853, 855 and 856 eV are associated with metallic Ni, NiO, and NiO interacting with supports, respectively [22,23]. Most of the surface Ni species were seemed to be oxidized due to the very weak peak assignable to metallic Ni. The reduced samples were exposed to air at room temperature when mounted on the sample holder. Thus it is expected that the oxygen layer on the surface of metallic Ni was easily formed by the exposure. In Fig. 8(b), the O 1s spectra of the three samples have a single strong peak at 530 eV, assignable to oxygen atoms in the Ti–O bond in TiO_2 lattice [24]. In Fig. 8(c), sharp and intense peaks at 459 and 465 eV were assignable to Ti $2p_{3/2}$ and Ti $2p_{1/2}$, respectively, indicating that the electronic state of titanium is mainly Ti^{4+}. In order to discuss the amount of exposed Ni species, the atomic ratios Ni/Ti are estimated from the following equation,

$$\frac{n_{\text{nickel}}}{n_{\text{titanium}}} = \frac{I_{\text{nickel}}/S_{\text{nickel}}}{I_{\text{titanium}}/S_{\text{titanium}}} \quad (4)$$

where n_x is the number of atoms per cm^3 of x element, I_x the intensity of peaks assignable to x element in XP spectra, and S_x the atomic sensitive factor of x element, as summarized in Table 1 [25]. As for the total amount of Ni species, the Ni/Ti ratios of fresh and employed Ni/TiO_2 were 0.090 and 0.054, respectively, which means that long-term operation at 200 °C decreased the amount of exposed Ni species on Ni/TiO_2. This result indicates that Ni particles sintered in the long-term operation. On the other hand, the Ni/Ti ratios of fresh and employed Ru–Ni/TiO_2 were 0.100 and 0.112, respectively, indicating no sintering of Ni particles.

3.3.4. Temperature programmed reduction by H_2

Fig. 9 shows the H_2-TPR profiles of the fresh and spent Ni/TiO_2, and as-prepared Ru–Ni/TiO_2. In Fig. 9(a), two sharp peaks at around 400 °C and 570 °C and one shoulder at more than 600 °C can be seen. Bokx et al. discussed the peaks using H_2-TPR technique for Ni/TiO_2 calcined at various temperatures [26]. The peak at the low temperature can be attributed to NiO reduction, whereas those at high temperatures (more than 500 °C) are assignable to the reduction of NiO strongly interacting with TiO_2 which Damyanova et al. defined as Ni^{2+} ion in $NiTiO_3$-like structure [27]. After the reduction of the fresh Ni/TiO_2 at 450 °C, a part of NiO still remained on the catalyst as evidenced by the weak and broad peak at ca. 600 °C in Fig. 9(b). For the employed samples, two broad peaks at low temperatures (250–550 °C) appeared in Fig. 9(c), and are assigned to the reduction of the surface oxygen layer on metallic Ni, in common with the result of XP spectra in Fig. 8(a). It is noteworthy that oxidized nickel species were diminished after the reduction of 7000 h-spent Ni/TiO_2 catalyst at 450 °C for 30 min, as confirmed by no peaks of NiO reduction in Fig. 9(d). As for as-prepared Ru–Ni/

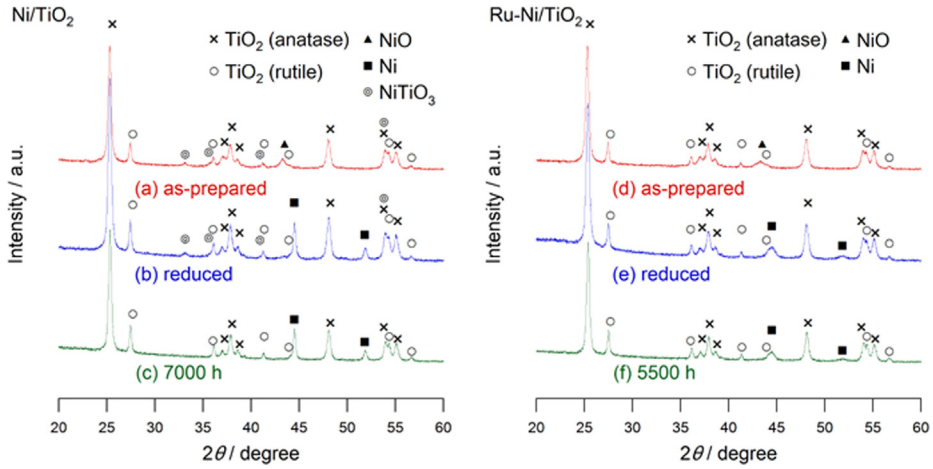

Fig. 6. XRD patterns of Ni/TiO_2 and Ru–Ni/TiO_2. (a) As-prepared Ni/TiO_2, (b) Ni/TiO_2 reduced at 450 °C, (c) Ni/TiO_2 after 7000 h of operation, (d) As-prepared Ni/TiO_2, (e) Ru–Ni/TiO_2 reduced at 450 °C, and (f) Ru–Ni/TiO_2 after 5500 h of operation JCPDS-card number: NiO (47-1049), Ni (04-0850), rutile-type TiO_2 (21-1276), anatase-type TiO_2 (65-5714), and $NiTiO_3$ (76-0334).

Table 1
Results of XP spectroscopy and XRD measurement for Ni/TiO_2 and $Ru–Ni/TiO_2$.

Catalysts		Area[a]		Ni/Ti	$D_{Ni(200)}$[c]/nm
		Ni $2p_{3/2}$ ($SF^b = 6.0$)	Ti 2p ($SF^b = 1.8$)		
10 wt%Ni/TiO_2	Fresh	1561	3060	0.090	22[d]
	7000 h	1286	3969	0.054	22
0.5 wt%Ru −10 wt%Ni/TiO_2	Fresh	2160	3582	0.100	7.3[d]
	5500 h	2522	3748	0.112	6.8

[a] Normalized by cumulative number of XP spectroscopy measurement.
[b] SF: sensitive factor [25].
[c] Estimated from a peak at 52° in XRD patterns.
[d] Reduced at 450 °C for 30 min.

TiO_2 (Fig. 9(e)), the reduction peak of NiO was shifted to lower temperature compared to the fresh Ni/TiO_2, indicating that the Ni reducibility was enhanced due to the presence of Ru. Dissociative hydrogen adsorption on a noble metal such as Ru, and the reduction of the neighboring metal oxides by such spillover hydrogen has been reported in our previous work and other reports [17,28]. The reduction of NiO by spillover H_2 from metallic Ru requires close contact of Ni species with Ru metal. For the spent $Ru–Ni/TiO_2$, two broad peaks at 200 and 400 °C appeared in Fig. 9(f). The peaks in Fig. 9(f) were located at lower temperature than those in Fig. 9(c), leading to high reducibility of Ni species on $Ru–Ni/TiO_2$ compared to Ni/TiO_2.

The difference in the catalytic performance between the fresh and spent Ni/TiO_2 is discussed here in relation with the

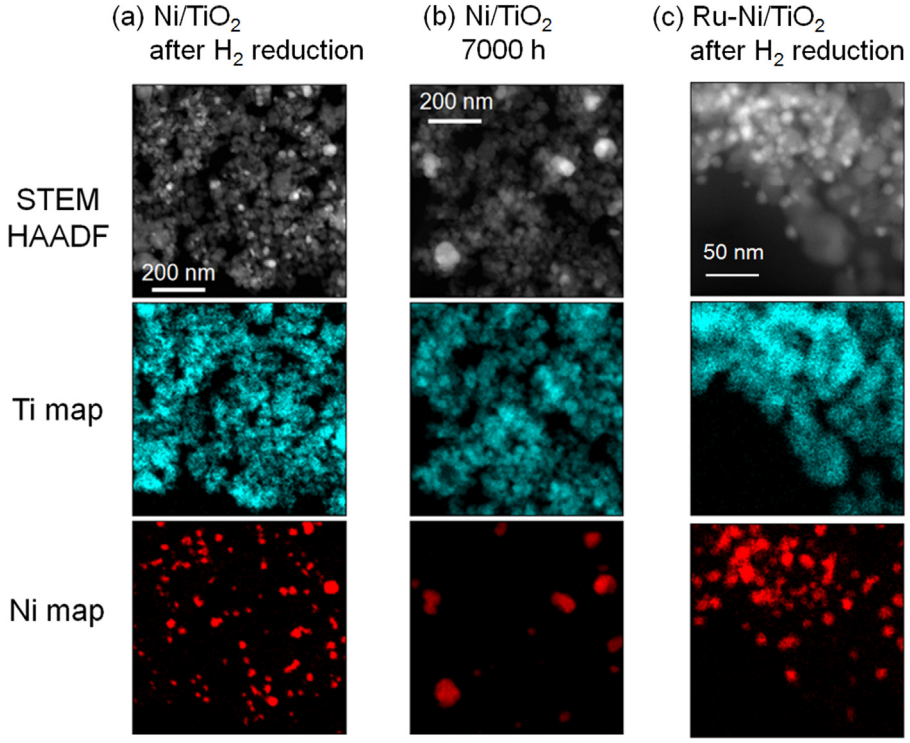

Fig. 7. STEM-HAADF images and Ti and Ni maps. (a) Ni/TiO_2 after H_2 reduction, (b) Ni/TiO_2 after 7000 h of operation, and (c) $Ru–Ni/TiO_2$ after H_2 reduction.

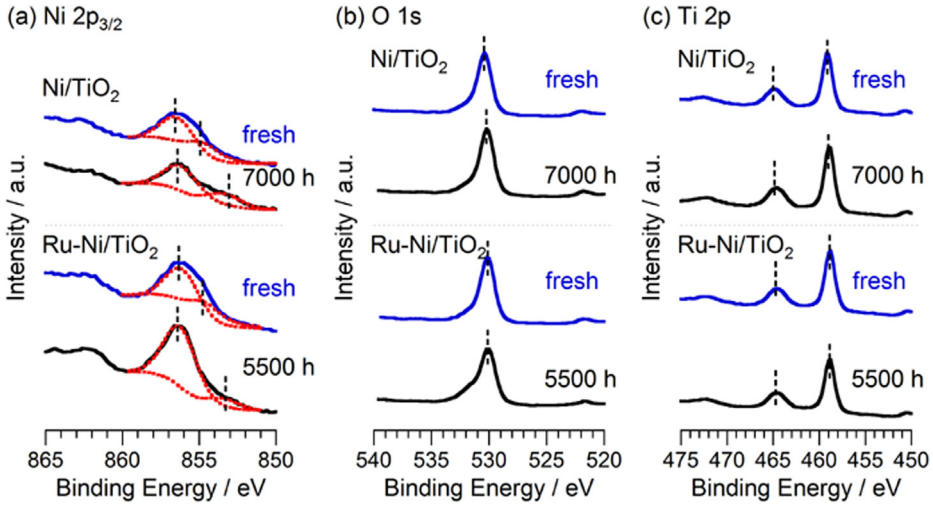

Fig. 8. XP spectra of (a) Ni $2p_{3/2}$, (b) O 1s, and (c) Ti 2p of Ni/TiO_2 and $Ru–Ni/TiO_2$. Samples: as-prepared Ni/TiO_2, employed Ni/TiO_2 for 7000 h, as-prepared $Ru–Ni/TiO_2$, and employed $Ru–Ni/TiO_2$ for 5500 h.

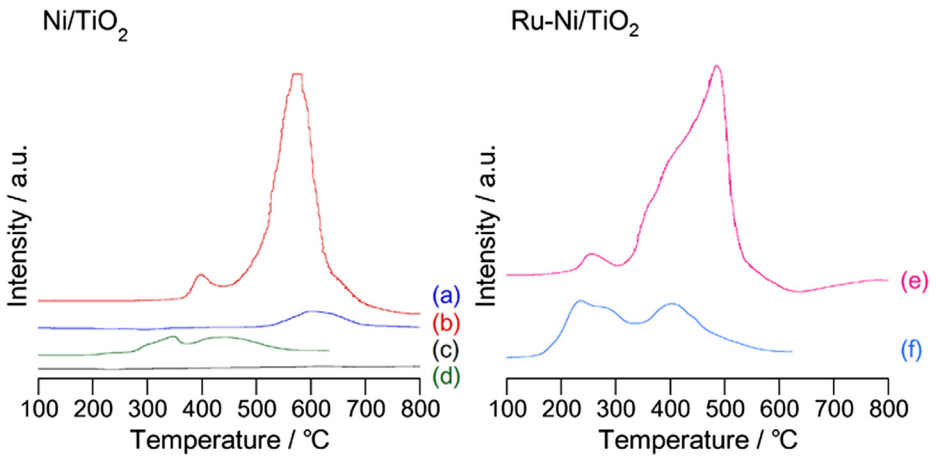

Fig. 9. H_2-TPR profiles of Ni/TiO_2 and $Ru–Ni/TiO_2$. (a) as-prepared Ni/TiO_2, (b) as-prepared Ni/TiO_2 reduced at 450 °C for 30 min, (c) 7000 h-spent Ni/TiO_2, (d) 7000 h-spent Ni/TiO_2 reduced at 450 °C for 30 min, and (e) as-prepared $Ru–Ni/TiO_2$. Heating rate = 10 °C min^{-1}.

characterization results as presented above. As shown in Fig. 3, CO_2 methanation activity over the spent catalyst was higher than that over the fresh one. The physical properties between these two catalysts were different in the following two points: 1) the long-term use slightly sintered Ni species on Ni/TiO_2, as indicated by STEM (Fig. 7) and XP spectra (Fig. 8), and 2) the result of H_2-TPR (Fig. 9) indicates that the selective CO methanation for 7000 h at 200 °C completely reduced the Ni oxides that remained unreduced after the pretreatment of the initial reduction at 450 °C. Provided that the slight sintering of the Ni species on Ni/TiO_2 is the main cause for the variation of the catalyst performance in the long-term test, the CO_2 methanation activity should be degraded since the active site for CO_2 methanation is the interface of Ni and support [29], which will be shortened as the Ni sintering proceeds. This is totally opposite to the activity change during the test, as shown in Fig. 3. As for the reduction of the remaining NiO species in the long-term test, prompt reduction of the NiO species can rapidly enhance the activity for CO_2 methanation. Furthermore, after the complete reduction of the NiO species CO_2 methanation activity should become stable. As shown in Figs. 2 and 4, the CO_2 methanation activity over Ni/TiO_2 and $Ru–Ni/TiO_2$ was improved from the very beginning of the long-term test, and successively got stabilized after 4000 and 2000 h of operation for Ni/TiO_2 and $Ru–Ni/TiO_2$, respectively. In addition, the duration of this transient period accords well with the reducibility of the NiO species on Ni/TiO_2 and $Ru–N/TiO_2$ as shown in Fig. 8. Therefore, the catalyst performance change in the long-term test can be derived from the reduction of NiO species, which improved the CO_2 methanation activity and consequently narrowed the temperature window for selective CO methanation.

3.4. Temperature window for selective CO methanation

As shown in Fig. 1, catalysts for selective CO methanation should possess wide temperature window located at a low temperature range so as to be employed in the commercial PEFC units. In addition, this window should remain wide during long-term operation. In order to specify the change in the temperature window of Ni/TiO_2 and $Ru–Ni/TiO_2$, the following two temperatures were plotted against time on stream in Fig. 10: the lowest temperature (T_{CO}) where CO concentration was <0.01%, and the highest temperature (T_{CH4}) where CH_4 concentration was <1%. The difference of T_{CO} and T_{CH4} was defined as the temperature window for selective CO methanation. As for both catalysts, T_{CO} was almost same during the tests. Over Ni/TiO_2, T_{CH4} was gradually dropped from 280 to 230 °C with increasing reaction time up to 4000 h, and then remained unchanged. For $Ru–Ni/TiO_2$, T_{CH4} was more rapidly decreased from 280 to 230 °C, and stayed constant after 2000 h. The stabilized temperature widow of Ni/TiO_2 was ca. 50 °C, and was almost same as that of $Ru–Ni/TiO_2$ (ca. 40 °C). It is noteworthy that $Ru–Ni/TiO_2$ maintained the wide temperature window for more than 5500 h at a high GHSV (10,000 h^{-1}), which means that $Ru–Ni/TiO_2$ is a promising catalyst for selective CO methanation in practical use.

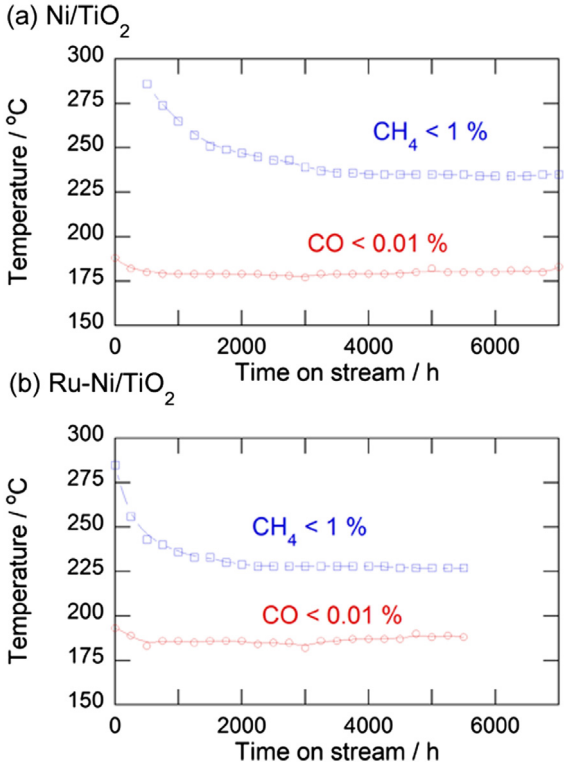

Fig. 10. Durability of (a) Ni/TiO_2 and (b) $Ru–Ni/TiO_2$ for selective CO methanation. Blue squares show the lowest temperature where CO concentration was below 0.01%, whereas red diamonds indicate the highest temperature where CH_4 concentration was below 1%. Reaction condition: $CO/CO_2/H_2/H_2O$ = 0.2/16.1/65.3/18.4. GHSV: (a) 2500 h^{-1} and (b) 10,000 h^{-1}.

4. Conclusions

Long-term tests of selective CO methanation was carried out over developed Ni/TiO_2 and $Ru–Ni/TiO_2$, and the durability was investigated. The performance of CO removal over $Ru–Ni/TiO_2$ was substantially superior to that of Ni/TiO_2. The $Ru–Ni/TiO_2$ displayed a wide temperature window of ca. 50 °C for more than 5500 h at a high gas hourly space velocity of 10,000 h^{-1}.

As for both catalysts, CO_2 methanation was boosted with increasing the time on stream in the long-term test due to an increase in the metallic Ni amount. In addition, the CO_2 methanation activity was stabilized after 4000 h (for Ni/TiO_2) and 2000 h (for $Ru–Ni/TiO_2$) of operation. The performance of both catalysts remained unchanged after this transient period during the long-term durability tests.

Acknowledgments

This study was supported by New Energy and Industrial Technology Development Organization (NEDO) (08002079-0 and 10000857-0).

References

[1] I. Staffell, R. Green, Int. J. Hydrogen Energy 38 (2013) 1088–1102.
[2] E. Antolini, J. Appl. Electrochem. 34 (2004) 563–576.
[3] E. Yoo, T. Okada, T. Kizuka, J. Nakamura, Electrochemistry 75 (2007) 146–148.
[4] T. Utaka, T. Okanishi, T. Takeguchi, R. Kikuchi, K. Eguchi, Appl. Catal. A Gen. 245 (2001) 343–351.
[5] P. Panagiotopoulou, D.I. Kondarides, Catal. Today 112 (2006) 49–52.
[6] O. Goerke, P. Pfeifer, K. Schubert, Appl. Catal. A Gen. 263 (2004) 11–16.
[7] M. Echigo, T. Tabata, Catal. Today 90 (2004) 269–275.
[8] F. Marino, C. Descorme, D. Duprez, Appl. Catal. B Environ. 54 (2004) 59–66.
[9] S.H. Kim, S.-W. Nam, T.-H. Lim, H.-I. Lee, Appl. Catal. B Environ. 81 (2008) 97–104.
[10] T. Tabakova, G. Avgouropoulos, J. Papavasiliou, M. Manzoli, F. Boccuzzi, K. Tenchev, F. Vindigni, T. Ioannides, Appl. Catal. B Environ. 101 (2011) 256–265.
[11] P. Panagiotopoulou, D.I. Kondarides, X.E. Verykios, J. Phys. Chem. C 115 (2011) 1220–1230.
[12] S. Eckle, Y. Denkwitz, R.J. Behm, J. Catal. 269 (2010) 255–268.
[13] A. Chen, T. Miyao, K. Higashiyama, H. Yamashita, M. Watanabe, Angew. Chem. Int. Ed. 49 (2010) 9895–9898.
[14] S. Takenaka, T. Shimizu, K. Otsuka, Int. J. Hydrogen Energy 29 (2004) 1065–1073.
[15] S. Tada, R. Kikuchi, K. Urasaki, S. Satokawa, Appl. Catal. A Gen. 404 (2011) 149–155.
[16] K. Urasaki, Y. Tanpo, T. Takahiro, J. Christopher, R. Kikuchi, S. Satokawa, Chem. Lett. 39 (2010) 972–973.
[17] S. Tada, R. Kikuchi, A. Takagaki, T. Sugawara, S.T. Oyama, S. Satokawa, Appl. Catal. B Environ. 140–141 (2013) 258–264.
[18] S. Tada, R. Kikuchi, A. Takagaki, T. Sugawara, S.T. Oyama, S. Satokawa, Catal. Today, http://dx.doi.org/10.1016/j.cattod.2013.09.048.
[19] S. Tada, D. Minori, F. Otsuka, R. Kikuchi, K. Osada, K. Akiyama, S. Satokawa, Fuel 129 (2014) 219–224.
[20] T. Inui, M. Funabiki, Y. Takegami, React. Kinet. Catal. Lett. 12 (1979) 287–290.
[21] W.H. Bragg, in: W.L. Bragg (Ed.), The Crystalline State, G. Bell and Sons Ltd., London, 1962, pp. 188–207.
[22] R. Yang, X. Li, J. Wu, X. Zhang, Y. Cheng, J. Guo, Appl. Catal. A Gen. 368 (2009) 105–112.
[23] S.R. Kirumakki, B.G. Shpeizer, G.V. Sagar, K.V.R. Chary, A. Clearfield, J. Catal. 242 (2006) 319–331.
[24] J. Yu, X. Zhao, O. Zhao, Thin Solid Films 379 (2000) 7–14.
[25] C.D. Wagner, L.E. Davis, M.V. Zeller, J.A. Taylor, R.H. Raymond, L.H. Gale, Surf. Interface Anal. 3 (1981) 211–225.
[26] P.K. de Bokx, R.L.C. Bonne, J.W. Geus, Appl. Catal. 30 (1987) 33–46.
[27] S. Damyanova, A. Spojakina, K. Jiratova, Appl. Catal. A Gen. 125 (1995) 257–269.
[28] J.-N. Park, E.W. McFarland, J. Catal. 266 (2009) 92.
[29] A.E. Aksoylu, Z. İlsenÖnsan, Appl. Catal. A Gen. 164 (1997) 1–11.